Extending the imaging volume for biometric iris recognition

Ramkumar Narayanswamy, Gregory E. Johnson,
Paulo E. X. Silveira, and Hans B. Wach

The use of the human iris as a biometric has recently attracted significant interest in the area of security applications. The need to capture an iris without active user cooperation places demands on the optical system. Unlike a traditional optical design, in which a large imaging volume is traded off for diminished imaging resolution and capacity for collecting light, Wavefront Coded imaging is a computational imaging technology capable of expanding the imaging volume while maintaining an accurate and robust iris identification capability. We apply Wavefront Coded imaging to extend the imaging volume of the iris recognition application.

OCIS codes: 100.5010, 100.2980, 170.0110.

1. Introduction

Recent interest in the use of biometric identification for security applications has led to the search for alternatives that are less error prone and less intrusive than traditional fingerprint identification. Among the alternatives, iris recognition is particularly attractive owing to the high degree of entropy per unit area encountered in human irises,[1] combined with the extremely small rate of change in human iris patterns with age and health conditions. For example, identical twins have completely distinct irises. The left-eye iris of a person bears no correlation with the right-eye iris. However, dynamic iris recognition presents some formidable challenges to the optical designer. To capture the iris information at the fidelity necessary for reliable identification, the optical system must maintain a high resolution over the entire field of view and depth of focus. Moreover, for robustness and ubiquity, the system should reliably identify subjects over an extended field of view and depth of focus.

Iris images as biometrics are currently being used for computer security (see Fig. 1 for an schematic example, or Panasonic's Authenticam for an example of a commercial implementation). In this application an iris recognition camera is typically mounted approximately 22 in. (1 in. = 2.54 cm) from the user. The iris system validates the user at the start of each session and may continue to validate at regular intervals. Some current commercial iris imaging systems, which operate at $F/8$, have an imaging volume of 3 in^3. (1 in. $\times$ 1.5 in. $\times$ 2 in.). This imaging volume is restrictive and not conducive for easy use. The user must be trained to use these types of systems and must actively cooperate every time his or her iris is to be validated. It is expected that increasing the imaging volume to 6 in. $\times$ 6 in. $\times$ 10 in., a factor-of-100 increase over the traditional imaging system, will make iris biometric recognition easier to use and more commercially acceptable. However, this increase in imaging volume must be achieved while maintaining recognition and rejection accuracy, which translates to the optical requirements of high imaging resolution and low F-numbers. The low-F-number requirement is also important for keeping the illumination intensity low enough to ensure eye safety under all conditions. These imaging-system characteristics are summarized in Table 1.

The field of view and the depth of field trade-offs required in traditional imaging systems can lead to impractical system designs. In traditional optical systems, increasing the field of view dictates that the imaging optics become significantly more complex, making it increasingly harder to control the aberrations that arise from imaging over large angular regions. The depth of field is typically increased by reducing the system aperture. However, smaller ap-

The authors are with CDM Optics, Inc., 4001 Discovery Drive, Suite 130, Boulder, Colorado 80303-7816. R. Narayanswamy's e-mail address is ramkumarn@cdm-optics.com.

Received 9 June 2004; revised manuscript received 13 October 2004; accepted 14 October 2004.

0003-6935/05/050701-12$15.00/0

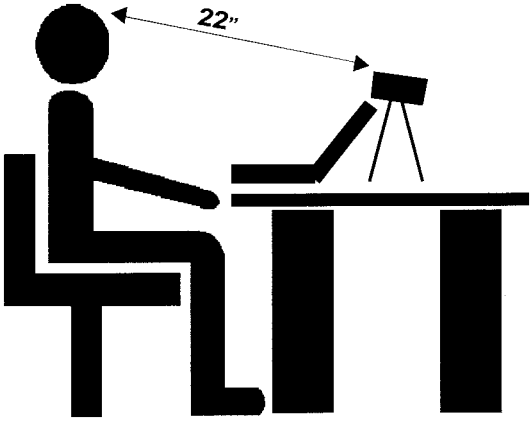

Fig. 1. Iris recognition system for computer security. An ideal iris recognition system captures and recognizes the iris accurately over a large imaging volume and requires no active cooperation from the user.

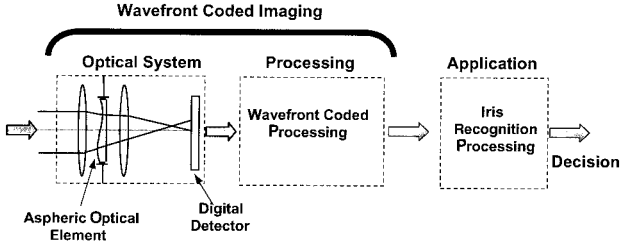

Fig. 2. Architecture of a computational imaging system consisting of application-specific optics and complementary signal processing. The optics and signal processing are jointly optimized for a particular imaging application.

ertures reduce the overall system resolution, which leads to loss of potentially valuable information in the higher spatial frequencies. Furthermore, a smaller aperture reduces the light-gathering capacity of the system. Reduction in light-gathering capacity is normally addressed by the use of longer integration periods or higher illumination levels. The former can lead to motion blur and the latter to eye-safety issues with active illumination. Thus the traditional approach leaves the optical system designer no other choice but to trade off resolution and light-gathering capacity for an increased depth of field.

Wavefront Coded imaging, a computational imaging method, can deliver a large field of view and depth of field without increasing the number of optical elements in the design or sacrificing the light-capturing capacity. Wavefront Coded systems consist of application-specific aspheric optical surfaces, followed by signal processing of the captured images. The specialized optics act as an encoder of the image information, and the signal processing acts as a decoder. The disadvantages of this type of imaging are a reduction in the signal-to-noise ratio (SNR) at best focus and the need to digitally process the acquired images. The former, as will be shown in this paper, is quite acceptable for biometric iris recognition, whereas the latter imposes a very small processing overhead in applications that require digital processing of the images, as is the case in iris recognition.

This paper is organized as follows. Section 2 provides a short introduction to the use of Wavefront Coded optics for extending the imaging volume of optical systems. Section 3 describes an iris recognition system and the system-design challenges that pertain to iris identification. Section 4 uses an off-the-shelf Wavefront Coded iris recognition system to experimentally show the benefits it offers over a traditional system for iris recognition. Section 5 explains in detail the design of an application-specific Wavefront Coded optical system that is optimized for an iris recognition algorithm and presents the results expected when an optimized design is used. Section 6 offers concluding remarks and points to areas of future research.

Table 1. Characteristics of an Ideal Imaging System for Iris Recognition

Characteristics
High iris recognition and rejection accuracy.
Ease of use—minimal user cooperation required.
Large image-capture volume.
High light-capture capacity (low $F/\#$, short exposure period).

2. Wavefront Coded Imaging

Wavefront Coded imaging is a novel imaging paradigm in which the optics and their complementary signal processing comprise an inherent aspect of imaging.[2,3] General Wavefront Coded imaging systems typically consist of specialized Wavefront Coded aspherical optics, a digital detector and a decoding or processing step, as shown in Fig. 2.

In iris imaging the optics are focused to the nominal object distance, and images of the scene are recorded exactly as in a traditional system. The detected image is processed with a decoding filter, which produces the decoded image. The decoding filter can be implemented through convolution, often derived from the point-spread function (PSF) of the Wavefront Coded imaging system. If the image recorded by the detector is examined before processing, it will appear as a blurred version of the eye. But the blur will be uniform across the image and will not vary as a function of field or object distances. This blurred image is an image optimized for information capture, as opposed to human visualization.

Figure 3 shows a comparison between the modulation transfer function (MTF) as a function of normalized spatial frequency (where unity represents the cutoff spatial frequency of the optical system) of a traditional system and a Wavefront Coded optical system at best focus (solid curve) and at an amount of defocus (dotted curve) arbitrarily selected but equally large in both plots. Note that, although the traditional (diffraction limited) optical system presents the largest MTF at all spatial frequencies [Fig. 3(a)], the MTF quickly degrades as a function of defocus and presents nulls at multiple frequencies, repre-

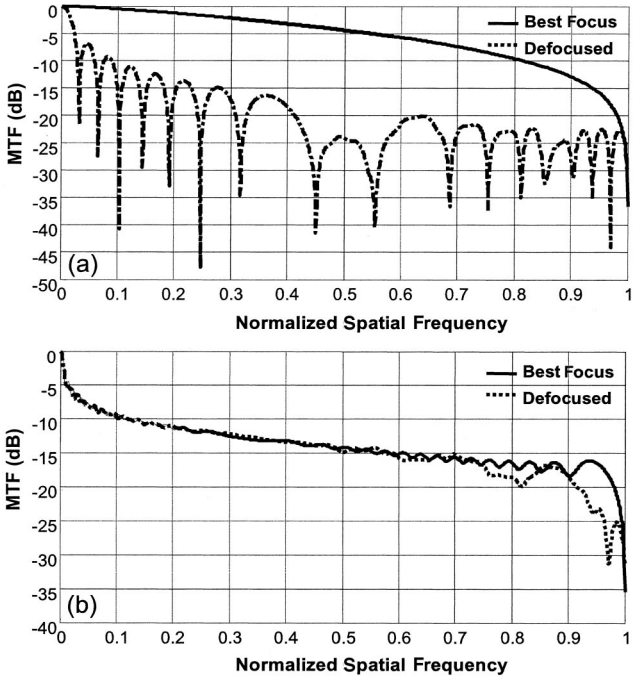

Fig. 3. Comparison between the modulation transfer function of (a) a traditional optical system and (b) a Wavefront Coded optical system. Notice that the traditional system has multiple nulls in the MTF, whereas the Wavefront Coded system maintains the system almost invariant with defocus. The same amount of defocus is applied in both cases.

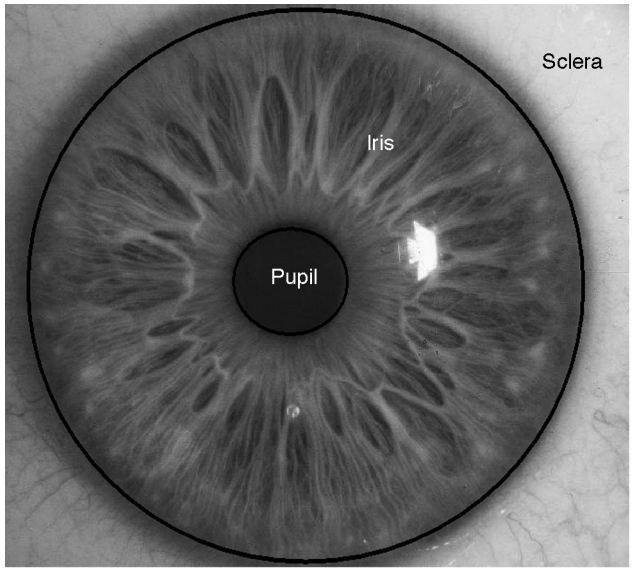

Fig. 4. Iris texture as a biometric. The rich texture of the iris differs significantly even between the left and the right eyes of the same person. This texture is encoded as a 2048-bit vector that forms the basis of the biometric.

senting the irremediable loss of information. In contrast, although the Wavefront Coded system [Fig. 3(b)] presents a lower MTF at best focus, it is capable of maintaining a nearly invariable MTF over a wide range of defocus. Moreover, no nulls are present in the intermediate spatial frequencies, allowing for full recovery of the image information after processing.

Wavefront Coding has been shown to effectively increase the depth of focus of numerous digital optical systems[4–10] and has been used for reducing the costs and increasing the robustness of optical systems by increasing their aberration tolerance.[11–14] Often, the primary consideration of these applications has been the visual quality of the images acquired, which is a subjective parameter. In this paper we demonstrate the benefits of using Wavefront Coded imaging in iris recognition, which represents a class of applications in which the performance metrics are quantitative, allowing for a nonsubjective analysis of the trade-offs of and advantages provided by Wavefront Coding.

3. Iris Recognition System

The visible part of the human eye consists of the pupil, the iris, and the sclera, as shown in Fig. 4. The color of the iris is of little use in recognition, but the texture of the iris is quite complex and unique. Even deeply pigmented irises, which appear black at visible wavelengths, show a rich texture with near-infrared (NIR) illumination. This rich iris texture has a significantly unique signature such that the operating probability of false acceptance can be of the order of 1 in 10^{10}. This false acceptance rate, which is a function of the decision threshold, can be changed to suit the specific application need, as described by Daugman.[1] Under realistic conditions, motion blur and noise may deteriorate the quality of the images available for comparison. Under these conditions, the threshold level may be reduced to reduce the false rejection rate at the expense of an increase in the false acceptance rate.

The use of the human iris as a means of identification has many advantages over other biometrics. Unlike fingerprints and the human face and voice, the iris remains unchanged over the majority of a person's life. From an operational perspective, the iris texture is attractive as a biometric owing to the possibility of imaging it from a distance: Cooperative users can be conveniently identified without much effort, and uncooperative users may be identified without their knowledge. Furthermore, the pupil has a physiological response to light, and the pupil's rapid diameter flutter acts as a natural test against artifice.

A. Functional Blocks of the Iris Recognition System

The iris recognition system can be functionally separated into the following blocks:

i. An infrared illumination system, which enables the imaging of the iris texture with good contrast. The illumination power level should be safe to the eye, but high enough to support short exposure periods.

ii. An imaging system, which acquires the image electronically for biometric processing. Ideally, the image should be free of defocus and aberration errors over a wide range of object distances and field positions and should facilitate reliable iris-score generation.

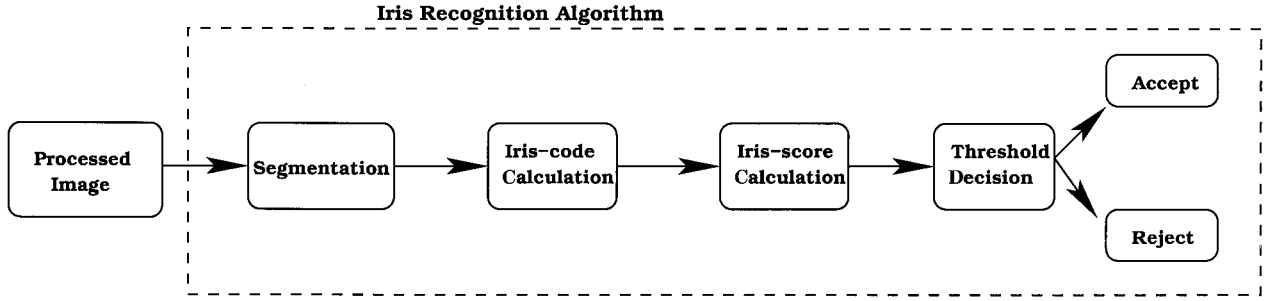

Fig. 5. Building blocks of the iris recognition algorithm. Wavefront Coding provides us with a processed image, which is segmented to separate the relevant parts of the iris. The iris code is computed from the segmented image and is compared with the database of iris codes, providing us with an iris score. A decision threshold step accepts or rejects the detected iris.

iii. An image-segmentation module, which locates the eye in the field of view and segments out the iris texture for signature analysis.

iv. An iris-score module, which converts the segmented texture into a series of binary codes.

v. A decision module, which compares the iris with a preexisting database and makes the accept or reject decision.

The modules for the iris-texture segmentation, iris-code calculation, iris-score calculation, and accept–reject decision typically constitute the iris recognition algorithm, as depicted in the diagram shown in Fig. 5. Although the main thrust of this research is the design of a specialized imaging system that is optimized for a particular iris recognition algorithm, a systemwide optimized design requires simultaneous optimization of the illumination system, the optics, and the multiple components of the iris recognition algorithm, because detailed knowledge of these modules helps to determine the precise specifications of the Wavefront Coded system.

B. Iris-Texture Segmentation

The iris-texture segmentation presented here is based largely on the research by Daugman[1] and Tisse *et al.*[15] The segmentation can be divided in two main steps. First, the eye is located in the field of view. Second, the pupil and iris boundaries are determined, and the iris texture is extracted and converted from an annulus into a rectangular image representation for further processing.

Figure 6 shows the results of locating the iris in the field of view and determining the pupil and iris boundaries. The iris and pupil centers can be located by use of the Hough transform, formulated for a circular object. The iris and pupil boundary radii are determined by the integrodifferential operator,[1]

$$\max(r,\ x_0,\ y_0)\left|\frac{\partial}{\partial r}\oint_{r,x_0,y_0}\frac{I(x,\ y)}{2\pi r}\,\mathrm{d}s\right|. \qquad (1)$$

This operator acts as a circular edge detector, and it operates by finding the values of the circle center $(x,\ y)$ and radius r that maximize the radial change of the line integral over all circles within the search range. The operator is used twice: first for finding the pupil–iris boundary and second for finding the iris–sclera boundary (see Figs. 4 and 6).

Once the iris and pupil boundaries are determined, the polar set of texture samples can be unwrapped into a rectangular grid by sampling in Φ evenly spaced angular steps and P evenly spaced radial steps between the pupil and the iris boundaries. Typically the iris texture tends to be stretched or squeezed, depending on the sampled pupil size. This remapping renders the iris texture uniform in size and makes it independent of the exact pupil radius at the time of imaging the eye. Figure 7 shows the iris texture from Fig. 6 remapped to a rectangular representation.

C. Computing the Iris Score

Portions of the iris texture that may be occluded by eyelids, eyelashes, and specular reflections are avoided. Although this leads to a potential loss in discriminating features, the high entropy present in the iris texture assures us that enough information is left by the unobstructed segments of the iris. Next the

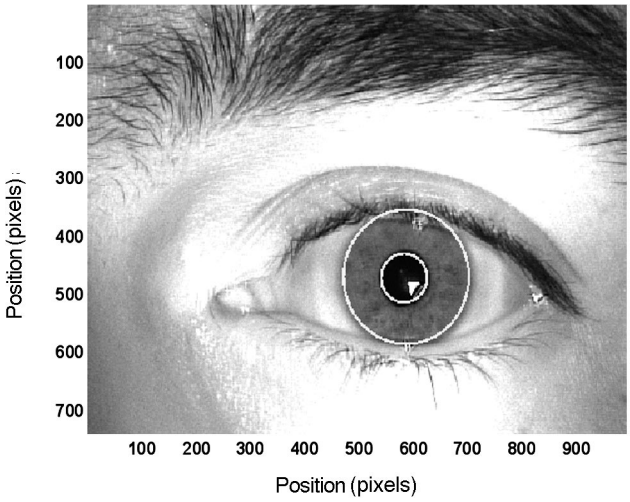

Fig. 6. Segmenting the iris texture in the image requires locating the eye in the image and precisely determining the pupil and iris boundaries. A slight error in localization can lead to dramatic performance degradation.

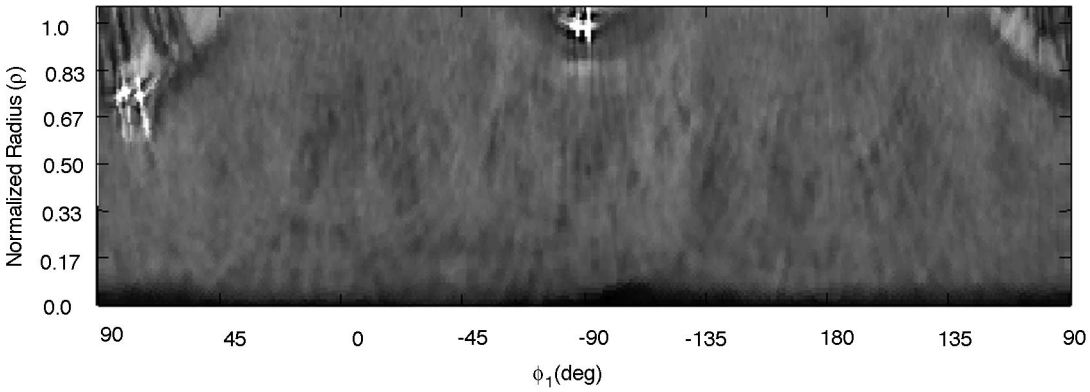

Fig. 7. Remapping the iris texture from an annular shape into a rectangular form.

segmented iris is processed by evaluation of the frequency content of the phase transitions of the iris patterns at various resolutions. Daugman[1] achieves this with complex two-dimensional Gabor wavelets. The resulting complex images have their real and imaginary parts thresholded to form the binary iris code. Following Tisse *et al.*,[15] we use bandpass filters and Hilbert transform the texture images, which are subsequently used to calculate the emergent phase and instantaneous frequency. Binary thresholding of the phase and frequency representations leads to the iris code.

Figure 8 shows the iris texture processed at three frequency bands thresholded about a preset value. Notice the gray-scale zebra-stripe pattern, which is characteristic of iris textures. This binary image is stored as a compact binary vector—varying in length from 2^{11} to 2^{14} bits—and composes the iris code.

The process of computing the iris score is a relatively simple matter of comparing the acquired iris code with the codes preenrolled in an iris database in a bit-by-bit fashion. Our iris recognition system, which is a variant of the algorithms described above, uses a normalized exclusive-NOR metric for bit comparison. The comparison of two images of the same iris results in a score close to 1, whereas the comparison of images of different irises results in a score close to 0. We use a decision threshold of 0.3, which we arrived at experimentally. An iris scoring above 0.3 is considered an acceptable match, whereas an iris scoring below 0.3 is rejected as a poor match.

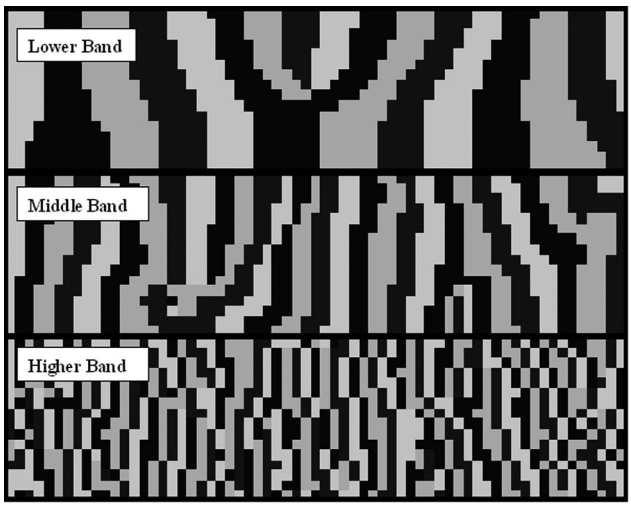

Fig. 8. Iris texture after filtering at three different passbands, after Hilbert transformation, and after thresholding. These filtered textures are used to derive the instantaneous frequency and emergent phase, which lead to the final iris score.

4. Extended Imaging Volume with Off-the-Shelf Wavefront Coded Optics

To provide us with proof of concept that Wavefront Coding can be effectively applied to iris recognition with an increased imaging volume, we built an optical system by using off-the-shelf Wavefront Coded optical components and compared its performance with that of a traditional optical system with similar components. By an "off-the-shelf" component we mean a commercially available Wavefront Coded optical element that is designed for generic depth-of-field applications, not optimized for iris recognition in particular.

Figure 9 shows a schematic diagram of the experimental setup used for capturing iris images over a range of distances. The setup uses a rail system actuated by a stepper motor. The optical system consists of a lens and a camera mounted on the rail system. In both the traditional and Wavefront Coded systems, the lens is a commercial 50-mm closed-

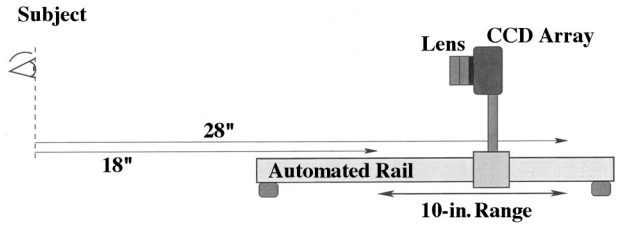

Fig. 9. Schematic diagram depicting the experimental setup used for automatically capturing iris images over a range of object distances. The lens can easily be changed, allowing us to use the same setup for characterizing traditional and Wavefront Coded optical systems.

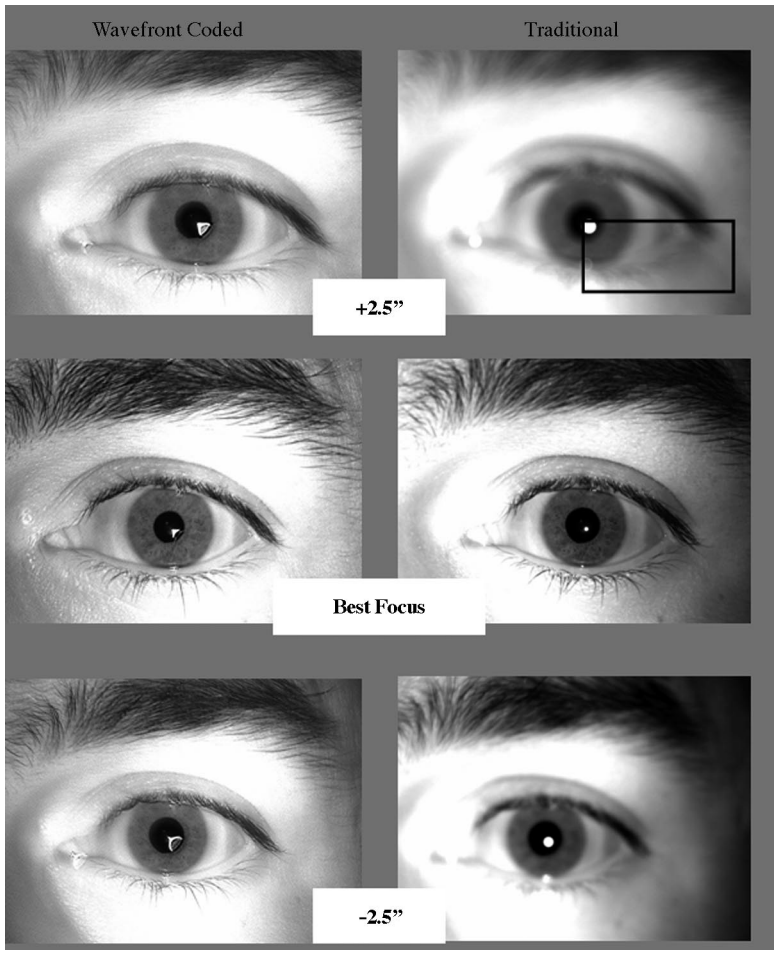

Fig. 10. Comparison between off-the-shelf Wavefront Coded imaging and traditional imaging. The value +2.5 in. indicates the object distance from the best-focus position toward the camera, and −2.5 in. indicates the object distance from the best-focus position away from the camera. Notice that the eyelashes are clearly resolved in the Wavefront Coded images, whereas they are lost in traditional imaging when the image is defocused.

circuit television (CCTV) lens set at $F/3.5$, and the camera is a 10-bit 1024 × 768 pixel CCD array. NIR illumination at 780 nm is provided by an array of four LEDs (not shown). The LEDs are pulsed so that they illuminate the subject's eye only during image capture, and the maximum intensity of the LEDs is limited so that the maximum exposure is always below the maximum eye-safety levels.[16] A computer synchronizes the rail motion, CCD image capture, and NIR illumination. Lenses attached to the CCD camera can easily be changed, allowing us to alternate between traditional and Wavefront Coded optics.

Iris images are captured from the left and right eyes of a cooperating subject at distances varying from 18 to 28 in. with 0.5-in. increments. Ten images are captured at every position, with a 1-s delay between images to allow for random variations in the position of the eye and eyelashes, as well as for variations in the size of the pupil. The Wavefront Coded images are processed, and the iris code is computed for each image.

Figure 10 compares iris images acquired with the traditional imaging system (right-hand side) and the off-the-shelf Wavefront Coded imaging system (left-hand side) at different object positions. These Wavefront Coded images were filtered by a Wiener filter designed to deconvolve the PSF of the Wavefront Coded system for human viewing. Signal processing for human viewing is not a requirement in general iris imaging. Note that the Wavefront Coded system is more capable of maintaining the details of the images at the defocused positions than is traditional imaging. These details can be better seen in the enlarged images shown in Fig. 11, in which we note that the eyelashes, eyebrow, and iris texture are much better resolved by the Wavefront Coded system, even though the image at best focus contains more artifacts than that obtained by the traditional system. Also note that an optimized Wavefront Coded system would have fewer artifacts and better iris recognition performance than this off-the-shelf Wavefront Coded system.

The images in Figs. 10 and 11 are provided only as visual references. The true test is in the examination of the iris scores as a function of object position. Figure 12 shows the iris scores for a traditional imaging

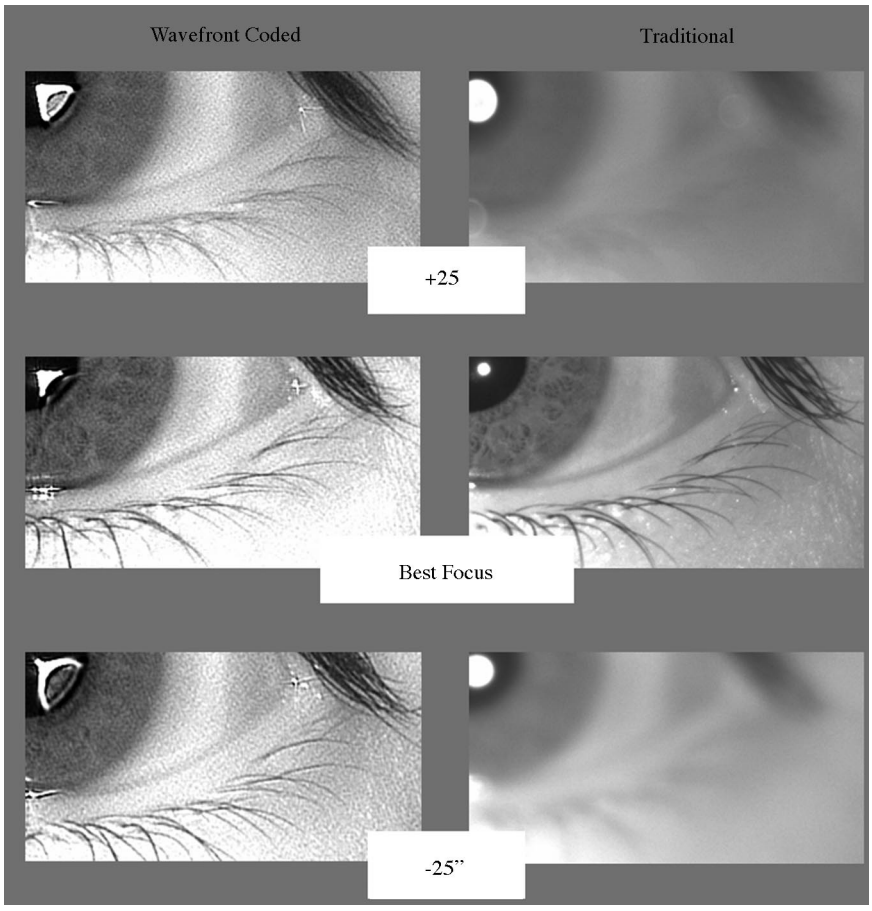

Fig. 11. Detailed view and comparison between the off-the-shelf Wavefront Coded images and the traditional images. Notice that the iris texture and eyelashes are well resolved in the Wavefront Coded images, whereas the traditional images lose these details except in the best-focus image.

system as a function of object distance. Each score is determined by averaging the score from 10 images taken at each position. The lens is focused at $z = 21.5$ in. and is not adjusted for focus as the camera moves with respect to the object. The reference iris was selected as the subject's left eye at best focus. Note that, at best focus, the iris score for the left eye (circles) is approximately 8.5 times higher than the score for the right eye of the same subject (diamonds), showing a high capacity for discriminating between the left and the right eyes. The dotted line highlights the minimum threshold for positive identification. Also note the sharp shape of the iris score, which indicates a shallow depth of field (approximately 3 in.). The plot indicates that the discrimination capacity at the best-focus position considerably exceeds system requirements. A system designer can view this excess as an opportunity to trade off this discrimination capacity for increased imaging volume, and Wavefront Coding is a tool capable of providing this trade-off.

Figure 13 shows the iris score for an off-the-shelf Wavefront Coded imaging system. The Wavefront Coded optical system consists of retrofitting a CCTV lens of the same model as that used in the traditional system with an off-the-shelf Wavefront Coded ele-

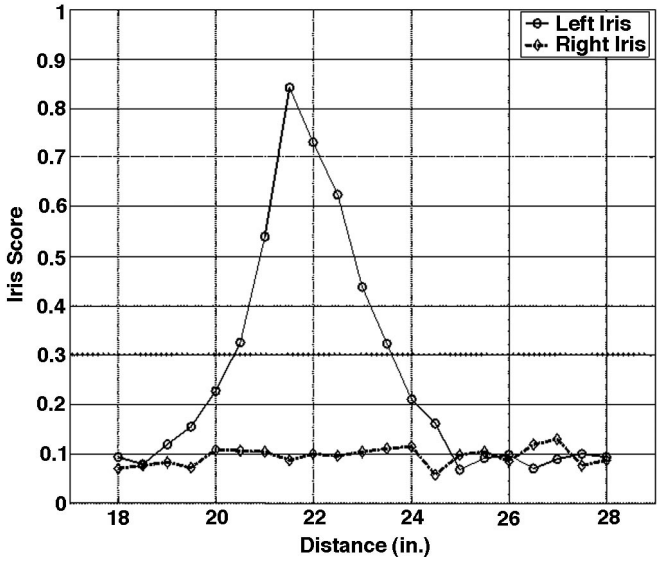

Fig. 12. Experimentally determined iris score of a traditional imaging system (non–Wavefront Coded system). The left eye has been enrolled into the database. The dotted curve shows the decision threshold used to discriminate valid score from invalid scores. The depth of field of the traditional system operating at $F/3.5$ is approximately 3 in.

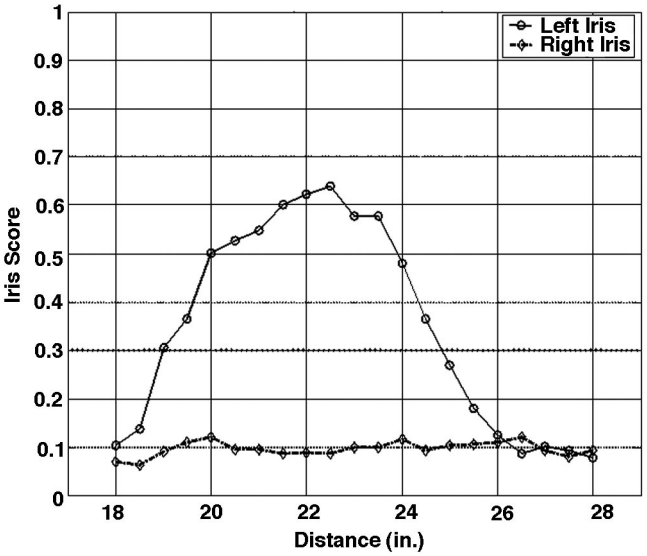

Fig. 13. Experimentally determined iris scores for an off-the-shelf Wavefront Coded system. These results are obtained by retrofitting a commercially available CCTV lens with an off-the-shelf Wavefront Coded element. Notice that the depth of focus has been increased to 6 in., which doubles the depth of focus of a traditional system.

ment. The element is a high-order separable aspheric element (explained in more detail in Subsection 5.B) with a total phase deviation of 57 wavelengths at a 546-nm wavelength. The reference iris is exactly the same as that used in the previous example (subject's left eye, captured with a traditional imaging system at best focus). Note that, in this case, the maximum ratio between the scores of the left and right eyes is reduced to 6.5, but the depth of field over which the iris score remains above the threshold level is extended to approximately 6 in., proving that the required trade-off can be effectively achieved. Nevertheless, the total range is still short of our desired goal, encouraging us to proceed with the design of a custom Wavefront Coded element that is optimized for iris recognition using the same CCTV lens.

5. Application-Specific Wavefront Coded Optical Design

This section describes the design of a custom Wavefront Coded optical element optimized for a specific signal processing task. This is done in contrast to what is typically done with traditional imaging systems in which the optical elements are designed with the goal of improving perceptual image visualization. The joint optimization in Wavefront Coded design is particularly relevant to applications in which the end result is not a subjective image quality perceived by the viewer but is a quantitative result that can be accurately measured. For example, in the iris recognition application, the overall system goal is to maintain the iris score above a preset threshold as the person's eyes move through the entire imaging volume. Given this overall application-level goal, subsystem-level metrics can be developed for the optical

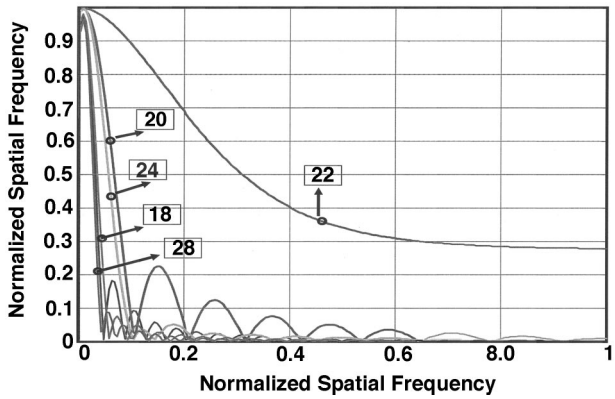

Fig. 14. MTF of the traditional CCTV system as it moves through focus. The numeric labels indicate the object distances (in inches; 1 in. = 2.54 cm) from the lens. Notice the MTF for the 22-in. best-focus position and compare it with the MTF at the other object distances. The MTF rapidly goes to zero for higher frequencies with increasing defocus.

system, the decoding filters, and the iris recognition algorithm.

A. Specifications for the Wavefront Coded Element Design

The fundamental goal of a Wavefront Coded imaging system is to maintain the MTF at a level significantly higher than the noise floor over a large imaging volume such that the relevant information can be extracted during postprocessing. Consider the MTF of the traditional iris-imaging optics at various object positions, as shown in Fig. 14. The MTF at 22 in. (best-focus position) has high modulation over the entire passband. However, the MTF curves drop rapidly as the system moves away from best focus. The contrast reversal frequency regions are separated by zero crossings, signifying an unrecoverable loss of information at those spatial frequencies. As discussed in Subsection 3.C, the iris recognition algorithm processes the iris texture at a number of specific frequency bands. Consequently, the optical system has a requirement to maintain the contrast across these frequency bands significantly higher than the noise floor over the imaging volume.

Wavefront Coded optics, along with decoding processing, has the added requirement of maintaining the position of the gray-to-white and white-to-gray transitions in the zebra-stripe pattern. Any processing that distorts the spatial relationship of the transitions results in an incorrect iris code. This requirement implies that the phase of the processed Wavefront Coded system's optical transfer function (OTF) cannot vary significantly over the imaging volume.

Digital processing of artifacts distorts the iris zebra-stripe transitions and lead to a reduced iris score. This implies that the processing filter should be optimized for minimum artifacts over the required imaging volume. The minimum contrast across spatial frequencies, maximum phase invariance, and maxi-

Table 2. Main Criteria for the Design of the Wavefront Coded Element and the Decoding Filters

Criteria
Maintain iris score above threshold and across imaging volume.
Maintain modulation in frequency bands of interest.
Maintain spatial relationship between edges in the iris texture.
Minimize the processing of artifacts.
Minimize the effects of aberrations.

mum processing of artifacts are cast as metrics for the optical design. Also, the CCTV lens prespecified for this application was originally designed for infinite conjugate imaging. Because we are using the lens for finite conjugate imaging, minimizing the spherical aberration over the field of view of the optical system is also a necessary requirement. Table 2 summarizes the main design requirements.

B. Designing the Wavefront Coded Element

The optical–digital imaging system is designed by use of WFCDesign, a customized imaging-system-design software package developed at CDM Optics and the primary tool for designing Wavefront Coded systems for a wide variety of applications.[17] This software allows for the simulation of the imaging system by combining optical ray tracing with a numeric model of the detector, followed by the signal processing necessary for decoding the image, followed by the application-specific signal processing (in this case, the iris recognition algorithm). The combination of all system parameters in one piece of software allows for the joint optimization of the optics and signal processing, constrained by the iris recognition algorithm. The optimized Wavefront Coded optics for the iris recognition application is built around the same commercial 50 − mm CCTV lens used in the off-the-shelf experiments, also operating at $F/3.5$. The front surface of the Wavefront Coding element is the optimized aspheric, whereas the rear surface is left flat. The typical requirements for the design and optimization of an imaging system include minimum modulation and maximum spot size or wave-front error at various conjugates. Wavefront Coded designs are also designed with minimum MTF requirements but are typically not constrained to wave-front error or spot size. Therefore the merit function is designed to penalize low modulation within the spatial frequencies of interest. This loss of contrast constituted the primary source of error for the optimizer and was given the highest weight in the merit function.

The optimizer uses the spot size as a metric to keep the PSF from becoming too large. It is necessary to constrain the size of the PSF in order to restrict the size of the specular reflection that originates from the illumination system. This is a concern because the spherical shape of the iris delivers a strong reflection that has a shape and size that are proportional to those of the PSF. The illumination level is set up to provide us with sufficient contrast in the iris texture, which typically requires the saturation of the pixels within the specular reflection. Thus a large specular reflection (large PSF) that spilled into the iris texture would corrupt the iris texture and thus reduce the area of the iris available for biometric identification.

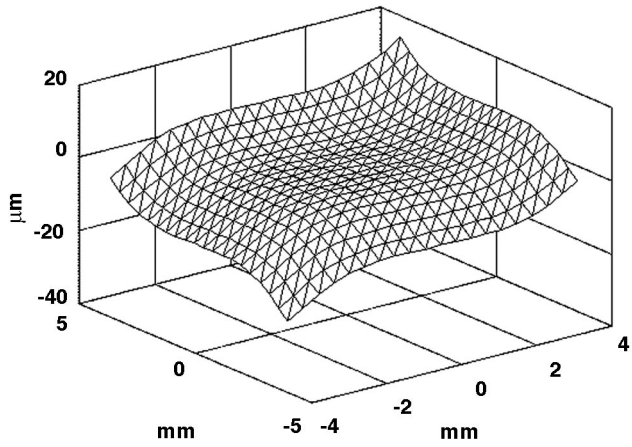

Fig. 15. Aspheric optical surface designed for iris recognition with a particular lens. The surface is approximately 40 μm from peak to valley. Adding this optical element to the 50-mm CCTV lens is expected to deliver a depth of field of 10 in., for an object distance ranging from 18 to 28 in.

Numerous designs were evaluated, and Fig. 15 shows the Wavefront Coded surface that delivered the best performance with respect to the specifications. The surface is derived from a family of phase functions specified by high-order separable polynomials. The phase surface is expressed as $P(x, y) = \exp\{-j[f(x) + f(y)]\}$, where $f(x)$ and $f(y)$ are high-order polynomials. The specific surface designed for this application is approximately 40 μm deep from peak to valley.

The surface will be molded in poly(methyl methacrylate) (PMMA), the material originally used to make hard contact lenses. The molding process requires a molding master that is the complement of the desired surface. The mold master is a diamond turned on a high-precision numerically controlled lathe with a fast tool servo. One mold master is machined for each side of the optical element. The PMMA material is injected by use of the mold master to deliver the Wavefront Coded element. The designed surface must meet various manufacturing requirements, including maximum slope and radius of curvature, and one of the surfaces is chosen to be planar for ease of manufacturing.

Figure 16 shows the MTFs for the 50-mm CCTV lens fitted with the designed aspheric–plano Wavefront Coded element. These MTFs should be compared with the traditional system's (non–Wavefront Coded) MTFs shown in Fig. 14. The absence of zeros in the MTF indicates that the information is retained in the Wavefront Coded image and can be extracted with suitable postprocessing. The sharp transitions in the MTFs are a consequence of the limited number of sampling points used to sample the PSFs in the spatial domain.

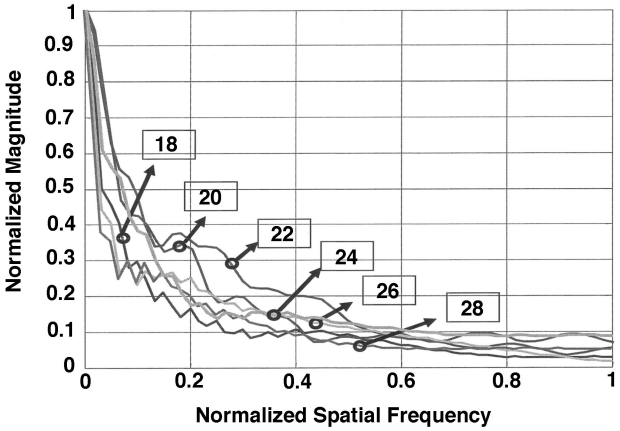

Fig. 16. MTFs of the Wavefront Coded system as a function of object distance (before processing). The numeric labels indicate the object distances in inches (1 in. = 2.54 cm). Notice that the MTFs do not have any zeros in the passband in contrast to the MTFs shown in Fig. 14 of the traditional imaging system. Absence of zeros in the MTF indicates that the information is retained in the Wavefront Coded image and can be extracted with suitable post-processing.

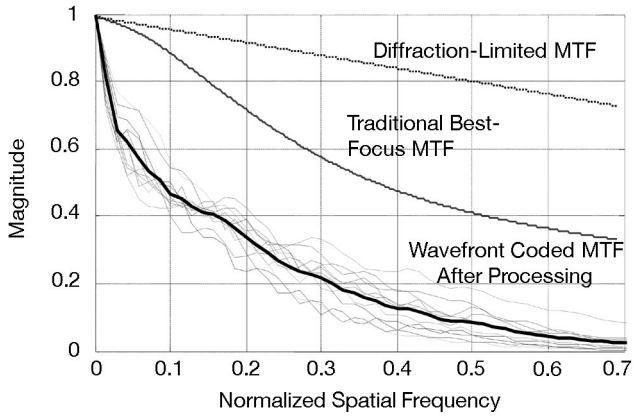

Fig. 18. MTFs of the custom Wavefront Coded system after processing compared with those of a traditional system (same optical system without Wavefront Coding) and of a diffraction-limited system at best focus. The processed system MTFs are parallel to the traditional best-focus MTF. The thick curve indicates the average processed response. The multiple curves around the average MTF represent processed MTFs at different object distances, spanning the range 18–28 in.

C. Designing the Wavefront Coded Decoding Filter

Typically, Wavefront Coded systems are designed to keep the PSF invariant across the imaging volume. This facilitates processing the Wavefront Coded images over the entire imaging volume by use of a single filter. However, two factors drive us toward using individual decoding filters at different object ranges. CCTV lenses are designed to image objects at infinity. Using this lens to image objects at distances of 18–28 in. leads to significant spherical aberration, as noted in Subsection 5.B. Our analysis noted that at the 18- and 28-in. positions the system encountered as much as 17λ of wave-front error. Typically, a λ/4 wavefront error is considered significant by optical designers.

We determined that three separate filters are adequate to process the images across the entire range of imaging volume, as depicted in Fig. 17. One filter spans the positions near best focus (19.5–23.5 in.), a second filter spans the middle positions (23.5–26.5 in.) and the third filter spans the ends, located at 18–19.5 in. and 26.5–28 in. Each image is processed with a specific filter based on the object distance D from the lens. This distance estimate can be calculated by measurement of the iris diameter, known to vary little across individuals, which averages approximately 11 mm.

Figure 18 shows the MTFs of the Wavefront Coded system after processing. In other words, these are the effective system MTFs of the Wavefront Coded system. Notice that these MTFs are all similar and are only a scaled version of the traditional best-focus MTF. The processed MTFs could be boosted to match the traditional best MTF, producing the high-contrast images that are often desirable for visual inspection. However, boosting the MTFs also boosts the number of processing artifacts in the images. For iris recognition, we have noted that it is more important to keep the artifact number low then to form high-contrast images. Alternatively stated, the contrast of the image is boosted just enough to obtain the best iris recognition performance while limited by the increase in the number of processing artifacts and the actual system noise.[18]

When an optical system is designed for imaging at best focus, the phase of the OTF is linear across all spatial frequencies within the passband of the sys-

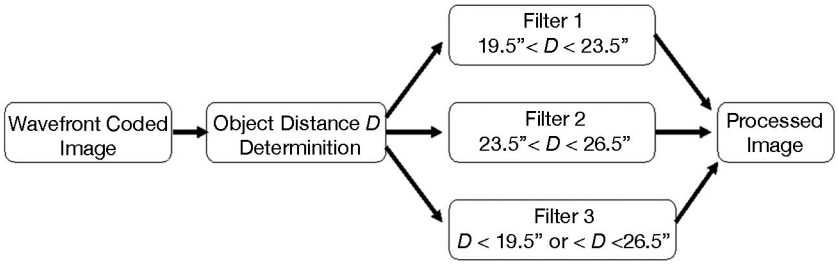

Fig. 17. Schematic representation of the selection process of decoding filter. The size of the iris is used to estimate the distance D to the object. One of three filters is selected, depending on the value of D. The processed image is obtained by filtering the raw image with the selected decoding filter.

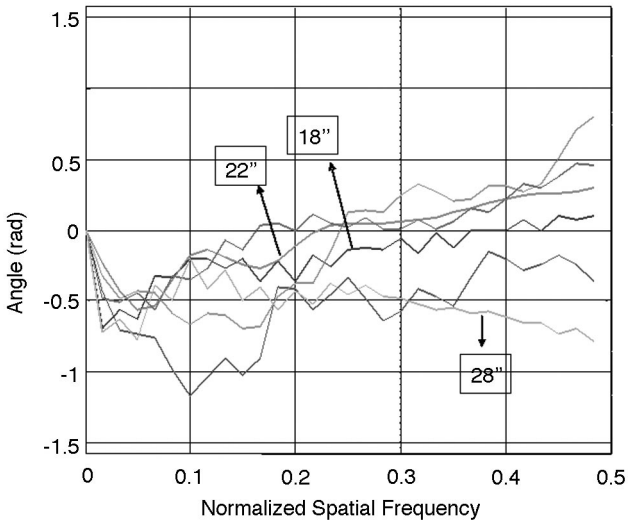

Fig. 19. Phase of the traditional OTF as the system moves through the entire imaging volume of 18 to 28 in. Notice that the phase variations are significant even within the lower frequencies, and they are not simply linear, which would result in only a spatial shift.

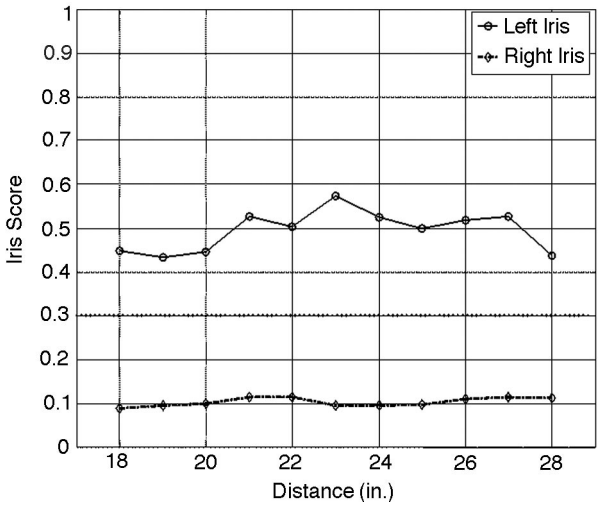

Fig. 21. Expected performance of the iris recognition system with the newly designed Wavefront Coded element fitted to the 50-mm CCTV lens. Note that the system is capable of recognizing the enrolled left eye over the entire distance, while rejecting the right eye. The depth of focus of this system is 10 in., which satisfactorily meets the specification of this application.

tem. Thus the phase of the OTF is usually ignored in those systems. As the system moves into the defocused regime, the phase of the OTF changes considerably and can no longer be ignored. Figure 19 shows the phase of the traditional optical system as it moves through the imaging volume. The phase errors are significant even within the lower frequencies, and they are not linear, resulting in image distortion.

Figure 20 shows the phase of the restored OTF for object positions ranging from 18 to 28 in. Notice that the phase is maintained within $\pm \pi/3$ up to the normalized spatial frequency of 0.5. This phase response is capable of decoding the iris zebra-stripe texture adequately in order to deliver acceptable iris scores. Thus Figs. 18 and 20 show that the Wavefront Coded system has adequately recovered the contrast and the phase of the spatial frequencies of interest, making them equivalent to what would be expected from a traditional imaging system at best focus.

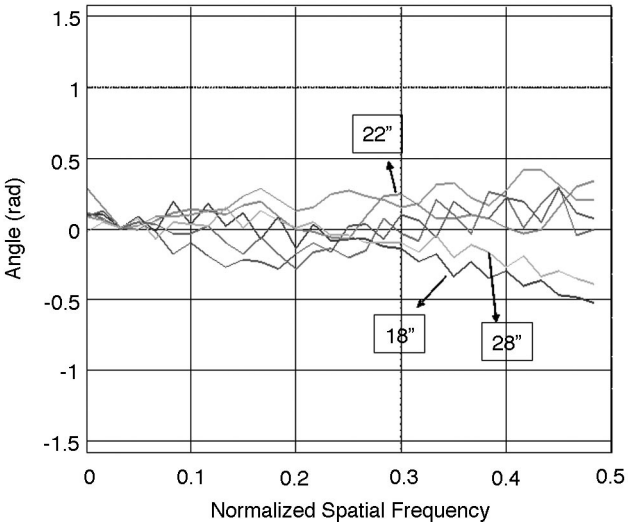

Fig. 20. One-dimensional phase of the Wavefront Coded optical system after processing, showing near-zero error in the region of spatial frequencies of interest. Maintaining a well-bounded phase difference at the lower frequencies is a requirement for correctly processing the zebra-stripe pattern in the iris texture.

D. Expected Imaging Volume with a Custom Wavefront Coded Optical Element

Figure 21 shows the expected performance of the iris recognition system with the custom Wavefront Coded element fitted to the 50-mm CCTV lens. Notice that the system is expected to accurately discriminate between the left and right irises through the entire 10-in. depth of field. Also note that the ratio between the score for the left iris (circles) has been reduced to about five times the score of the right iris (diamonds), providing us with quite a large increase in the depth of field with a small penalty in iris score compared with the off-the-shelf Wavefront Coded optical system (6-in. depth of field for a 6.5 ratio in scores) or with the traditional system (3-in. depth of field for an 8.5 ratio in scores). Thus we see that Wavefront Coding allows us to effectively trade off the peak iris score for a wider discrimination range. From an optical-system point of view, Wavefront Coding allows the designer to trade off the peak SNR at best focus for an SNR that is higher than a specified threshold over an extended imaging volume.

These simulations are obtained starting from a high-resolution iris image captured at best focus with a traditional optical system. This image is then convolved with the PSF of the designed optical system at each object distance and sampled in such a way as to mimic actual imaging and detection. Simulated detection noise is added to the image, which consists of

signal-independent read noise and signal-dependent shot noise, providing us with simulated raw images. The images are then filtered with one of the decoding filters corresponding to its object distance, providing us with the postprocessed image. Then the image is segmented, its iris code is extracted, and an iris score is assigned to the image, providing us with the data shown in Fig. 21.

6. Conclusion and Future Research

Wavefront Coded imaging has been shown to increase the imaging volume for the iris recognition application. Off-the-shelf Wavefront Coded optical components were used to experimentally prove the imaging volume extension and successful iris recognition. However, off-the-shelf components did not deliver the desired 10-in. depth of field desired, leading us to the design of an application-specific Wavefront Coded element. Simulation results with the optimized element indicate accurate iris discrimination over 10 in. This paper discussed in detail the design of this application-specific optical element, which included optimization over the imaging system and decoding filter for a given iris recognition algorithm.

Fabrication of the custom Wavefront Coded optical element is currently underway. Future research includes testing and measuring the fabricated element, along with conducting extensive experimental tests, to show in a statically significant manner that Wavefront Coded imaging does increase the imaging volume while maintaining effective discrimination in iris recognition.

The desired imaging volume for this application is 6 in. $\times$ 6 in. $\times$ 10 in., where the maximum field of view is 6 in. $\times$ 6 in. and the depth of field is 10 in. The 10-in. depth of field has been demonstrated in the simulations, but the current imaging system with a 1/3-in. sensor has a maximum field of view of 3 in. $\times$ 3 in. The next-generation system will use a 2/3-in. sensor to deliver the desired 6 in. $\times$ 6 in. field of view. Simulations indicate that the system performs well for nonaxial field positions, so moving to a large field of view should readily be achieved with the custom Wavefront Coded element being fabricated.

As part of this future experimental research, receiver operating curves, which plot the probability of detection with respect to false positives, will be plotted while varying the parameters associated with the imaging system (illumination, exposure, and sensor gain), Wavefront Coded processing, and iris algorithms (decision threshold and width of bandpass filters). Multiple iris recognition algorithms will be evaluated, and one will be chosen for the next-generation system.

The authors would like to acknowledge valuable discussions with Joe van der Gracht of HoloSpex, Robert J. Plemmons of Wake Forest University, and Michael C. King of the U.S. Department of Defense. ST Microelectronics provided the iris recognition software and valuable insight into their algorithm. This study was accomplished with the support of the Army Research Office under Department of Defense grant DAAD19-00-1-0540.

References

1. J. G. Daugman, "High confidence visual recognition of persons by a test of statistical independence," IEEE Trans. Pattern Anal. Mach. Intell. **15,** 1148–1161 (1993).
2. S. Prasad, T. Torgersen, V. P. Pauca, R. J. Plemmons, and J. van der Gracht, "Restoring images with space variant blur via pupil phase engineering," special issue on computer imaging, Opt. Inf. Syst. **4,** 4–5 (2003).
3. J. N. Mait, R. Athale, and J. van der Gracht, "Evolutionary paths in imaging and recent trends," Opt. Exp. **11,** 2093–2101 (2003); http://www.opticsexpress.org.
4. R. Narayanswamy, A. E. Baron, V. Chumachenco, and A. Greengard, "Applications of wavefront coded imaging," in *Computational Imaging II*, C. A. Bouman and E. L. Miller, eds., Proc. SPIE **5299,** 163–174 (2004).
5. S. Bradburn, E. R. Dowski, Jr., and W. Thomas Cathey, "Realizations of focus invariance in optical–digital systems with wave-front coding," Appl. Opt. **36,** 9157–9166 (1997).
6. J. van der Gracht, E. R. Dowski, W. T. Cathey, and J. Bowen, "Aspheric optical elements for extended depth of field imaging," in *Novel Optical System Design and Optimization*, J. M. Sasian, ed., Proc. SPIE **2537,** 279–288 (1995).
7. E. R. Dowski and W. T. Cathey, "Extended depth of field through wave-front coding," Appl. Opt. **34,** 1859–1866 (1995).
8. S. C. Tucker, E. R. Dowski, and W. T. Cathey, "Extended depth of field and aberration control for inexpensive digital microscope systems," Opt. Exp. **4,** 467–474 (1999); http://www.opticsexpress.org.
9. A. E. Baron and V. V. Chumachenko, "An alternative approach to optical imaging," IVD Technol. **8,** 47–51 (2002).
10. W. Cathey and E. Dowski, "New paradigm for imaging systems," Appl. Opt. **41,** 6080–6092 (2002).
11. E. R. Dowski, R. H. Cormack, and S. D. Sarama, "Wavefront coding: jointly optimized optical and digital imaging systems," in *Visual Information Processing IX*, S. K. Park and Z.-U. Rahman, eds., Proc. SPIE **4041,** 114–120 (2000).
12. H. B. Wach, E. R. Dowski, and W. T. Cathey, "Control of chromatic focal shift through wave-front coding," Appl. Opt. **37,** 5359–5367 (1998).
13. E. R. Dowski, Jr., S. C. Bradburn, and W. T. Cathey, "Aberration invariant optical/digital incoherent systems," Jpn. Opt. Rev. **3,** 492–432 (1996).
14. E. R. Dowski, A. R. FitzGerrell, and W. T. Cathey, "Optical/digital aberration control in incoherent optical systems," in *Second Iberoamerican Meeting on Optics*, D. Malacara-Hernandez, S. E. Acosta-Ortiz, and R. Rodriguez-Vera, eds., Proc. SPIE **2730,** 120–126 (1995).
15. C. Tisse, L. Martin, L. Torres, and M. Robert, "Person identification technique using human iris recognition," *Proceedings of the 15th International Conference on Vision Interface* (n.p., 2002), pp. 27–29.
16. C. P. Cain, D. Courant, D. A. Freund, B. A. Grossman, P. A. Kennedy, D. J. Lund, M. A. Mainster, A. A. Manenkov, W. J. Marshall, R. McCally, B. A. Rockwell, D. H. Sliney, P. A. Smith, B. E. Stuck, S. A. Tell, M. L. Wolbarsht, and G. I. Zheltov, "Revision of the guidelines on limits of exposure to laser radiation of wavelengths between 400 nm and 1.4 μm," Health Phys. **79,** 431–440 (2000).
17. K. Kubala, E. Dowski, and W. Cathey, "Reducing complexity in computational imaging systems," Opt. Exp. **11,** 2102–2108 (2003); http://www.opticsexpress.org.
18. F. O. Huck, C. L. Fales, N. Halyo, and K. Stacy, "Image gathering and processing: information and fidelity," J. Opt. Soc. Am. A **2,** 1644–1666 (1985).